Ultrafast laser-induced electron emission from multiphoton to optical tunneling

M. Pant[1] and L. K. Ang[1,2,*]

[1]*School of Electrical and Electronic Engineering, Nanyang Technological University, Singapore 639798*

[2]*Singapore University of Technology and Design, Singapore 138682*

(Received 25 January 2012; revised manuscript received 9 May 2012; published 16 July 2012)

Based on a time-dependent quantum model, a relation between the onset of the optical tunneling regime and the metal work function is determined. In the multiphoton regime, the number of photons required for absorption is reduced from $n = 3$ (at pulse length $\tau > 20$ fs) to $n = 2$ (at $\tau < 8$ fs) due to the energy uncertainty principle. The phase of the laser is important for optical tunneling, but is only manifest in the multiphoton regime when the number of laser cycles is close to or less than 1. The effect of the field gradient at the tip can be important when the radius of the tip is 40 nm or smaller. The extension of the model to include nonequilibrium electron distribution due to ultrafast laser excitation is discussed. Comparisons with other models and experimental findings are presented.

DOI: 10.1103/PhysRevB.86.045423 PACS number(s): 79.70.+q, 41.75.−i, 79.20.Ws, 79.60.−i

I. INTRODUCTION

The emission mechanism[1–12] of femtosecond laser-induced electron emission from a DC-biased sharp metallic tip has attracted considerable interest in recent years due to its applications in various ultrafast electron imaging methods, which are able to provide ultrafast time-resolved information about the underlying dynamics of many processes in physics, chemistry, and biology.[13] The underlying electron emission mechanism is difficult to pin down quantitatively as the emission occurs in the transition region with a Keldysh parameter $\gamma = \omega\sqrt{2m\Phi}/eE$ of order 1, which is between the multiphoton ($\gamma \gg 1$) and tunneling ($\gamma \ll 1$) regimes. In this regime, the tunneling time is comparable to or smaller than the characteristic time scale of the ultrafast laser pulse. Compared to the time-independent general electron emission model,[14] there has been some debate between the pioneering experiments proposing different mechanisms, such as optical field emission[2] ($\gamma = 3$ to 9), multiphoton field emission[3] ($\gamma \approx 4$), and multiphoton absorption followed by over-barrier emission[4] ($\gamma = 3$ to 4). Subsequent studies in the area include nonequilibrium multiphoton emission models ($\gamma > 1$),[5–7] strong photoemission ($\gamma \approx 2$),[8,9,12] above-threshold photoemission ($\gamma \approx 3$ to 5),[10] and attosecond electron pulses ($\gamma \approx 2$).[11] In addition to the cited recent works above, some earlier studies in this area include the analysis of emission sensitivity from gold,[15] the theory of ultrashort nonlinear multiphoton photoelectric emission,[16] the dependence of the photoelectric effect on the dynamic electron distribution function,[17] and the simultaneous measurements of second-harmonic generation and two-photon photoelectric emission from gold.[18]

Recently, a smooth transition from multiphoton to optical tunneling has been shown experimentally using a 30 fs, 830 nm ultrafast laser on a good tip[8] for which the transition is calculated to occur at a laser field of around 9 to 10 V/nm ($\gamma \approx 2$).[9] It is of interest to obtain a simple scaling law or formula that can calculate the required laser field or critical Keldysh parameter at the transition over a wide range of laser parameters (wavelength, pulse length, and phase angle) and material properties (work function and image charge potential).

Keldysh theory has shown that the transition between the two regimes is smooth and it is dependent on which quantity, such as total rate, energy spectrum, or angular distribution, one uses in the study of the transition. To avoid any confusion, in our paper presented here, we define the critical Keldysh parameter as the *onset* of the optical tunneling regime for which the amount of electron emission cannot be expressed by the power law of the multiphoton regime with a scaling of emitted charge proportional to F_0^{2n}, where F_0 is the laser field and n is the number of photons absorbed per electron. Under this definition, the onset condition proposed and calculated in this paper can be viewed as the lower bound of the transition between the multiphoton and tunneling regimes.

Before presenting the results, we would like to present a short summary of the findings reported in this paper: (a) Based on the scaling of the emitted charge with the laser field, an analytical expression to determine the critical Keldysh parameter at the onset of the optical tunneling regime has been obtained (see Figs. 1 and 2). (b) In the multiphoton regime, the number of photons required for multiphoton absorption depends on the laser pulse length if the work function is not close to a multiple of the photon energy. For example, we predict that $n = 3$ multiphoton emission at long pulse (>20 fs) can be reduced to $n = 2$ at short laser pulse (<8 fs), as shown in Fig. 3. (c) The effects of laser phase and pulse length are studied in detail in Figs. 4 and 5. (d) A comparison of the calculated results with different radii of the tip to account for the effects of the field gradient is shown in Fig. 6. (e) Comparisons of our model with a recent model and experimental measurement are presented, respectively, in Figs. 7 and 8.

The time-dependent quantum tunneling model is presented in Sec. II. The results of the critical Keldysh parameter, pulse-length dependence of multiphoton absorption, and effects of laser parameters are presented, respectively, in Secs. III, IV, and V. Comparison with prior works and effects of the field gradient and nonequilibrium ultrafast laser excitation are discussed in Sec. VI. Finally, we conclude our paper in Sec. VII.

II. TIME-DEPENDENT QUANTUM TUNNELING MODEL

Consider a one-dimensional (1D) model with the metal-vacuum interface at $x = 0$. The potential energy inside the

metal ($x < 0$) is a negative constant U_m with respect to the vacuum energy level defined as zero. The potential energy in the vacuum region ($x \geqslant 0$) is

$$U(x,t) = -\frac{e^2}{16\pi\epsilon_0(x+x_0)} - ex\Bigg[F_{\rm DC} + F_0 \exp \times \left(-2\ln 2\frac{(t-t_0)^2}{\tau^2}\right)\cos[\omega(t-t_0)+\phi]\Bigg], \quad (1)$$

where $F_{\rm DC}$ is the applied DC field, F_0 is the peak of the laser field envelope, τ is the laser pulse length, ϕ is the laser phase angle, and $\omega = 2\pi c/\lambda$ is the laser angular frequency (λ is the laser wavelength, c is the speed of light). Here t_0 (set at 40 fs) is a reference point at the center of the laser pulse, and $x_0 = -e/[16\pi\epsilon_0 U_m]$ is a value selected to have a continuous potential at the interface.

The initial wave function is obtained by first solving the time-independent Schrödinger equation in the absence of any applied field ($F_0 = F_{\rm DC} = 0$). Knowing that the initial wave function must approach zero as x approaches infinity, it can be expressed as $\Psi_0(x<0) = C_1\sin(k_m x) + C_2\cos(k_m x)$ and $\Psi_0(x \geqslant 0) = C_3 W_{a/2\sqrt{b},-1/2}(2\sqrt{b}(x+x_0))$, where $k_m = \sqrt{2m(E-U_m)}/\hbar$, $W_{k,m}(x)$ is the Whittaker W function, $a = e^2m/(8\hbar^2\pi\epsilon_0)$, and $b = -2Em/\hbar^2$. For electron tunneling, the probability of tunneling drops rapidly with decreasing electron energy and most of the emitted electrons are expected to be from a source near the Fermi level. Thus, we assume that the energy of the electron source is at $E = -\Phi_m$, where Φ_m is the work function of the metal.

Since only the electrons near the Fermi energy level participate in the emission process, only a fraction k_BT/E_F of the total electron density is assumed to contribute to the emission current at room temperature $T = 300$ K, where $E_F = -\Phi_m - U_m$ is the Fermi level relative to the metal potential energy U_m. For tungsten, we have $\Phi_m = 4.5$ eV, $U_m = -13.5$ eV, and $E_F = 9$ eV.

Using the initial wave function Ψ_0, we numerically solve the time-dependent Schrödinger equation to calculate the wave function $\Psi(x,t)$ for a given set of parameters $F_{\rm DC}$, F_0, τ, ϕ, and ω. The wave function is monitored at a distance of 2 nm from the interface to determine the time-dependent current density $J(t)$. The total emitted charge density σ is calculated by the time-integration of $J(t)$. The dependence of σ and $J(t)$ on various parameters will be discussed in the following figures. Unless specified, the default value of the laser phase angle is $\phi = 0$ and the DC field is $F_{\rm DC} = 0.2$ V/nm. Here, both $F_{\rm DC}$ and F_0 are assumed to include the field enhancement factor. In the calculation of the Keldysh parameter, we have ignored $F_{\rm DC}$ as it is at least 20 times smaller than the laser field F_0 in the transition to the optical tunneling regime.

In our model, the numerical constants in Ψ_0 are determined by using the appropriate density of electrons contributing to the emission process and by matching the continuity equations at the metal-vacuum interface. The calculated results at zero laser field condition ($F_0 = 0$) are then verified by using the classical field emission model: Fowler-Nordheim (FN) law based on the 1950's Murphy and Good formulation. Although there are a number of approximations in the FN law, our model shows good agreement in the range of $F_{\rm DC} = 2.5$ to 4 V/nm.

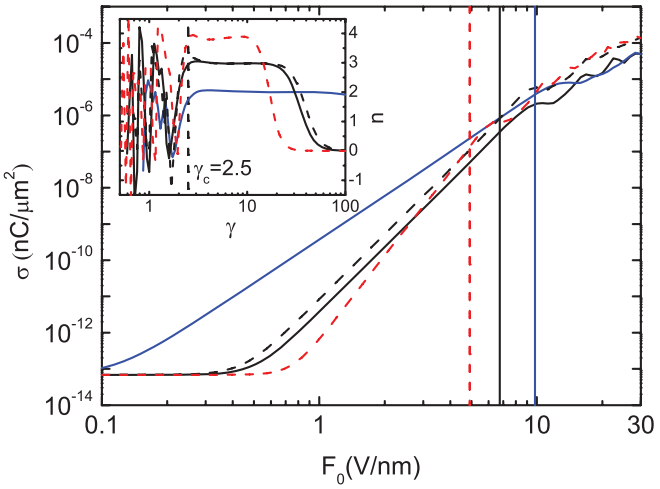

FIG. 1. (Color online) Dependence of the emitted charge density σ on the laser field F_0 for λ (nm) = 550 (blue), 800 (black), and 1100 (red) from top to bottom at low F_0 and pulse length τ (fs) = 8 (solid) and 20 (dashed). The vertical lines indicate the critical value of F_0 at the transition from multiphoton to optical tunneling regime. The inset shows the plot of n vs γ.

III. ONSET OF OPTICAL TUNNELING EMISSION

As mentioned earlier, our model is able to provide an analytical expression for the onset of optical tunneling emission where the power-law scaling of multiphoton emission (see below) becomes invalid. In this section, we will present the numerical results that will eventually lead to the analytical expression.

In Fig. 1, the time-integrated charge density σ is plotted as a function of peak laser field F_0 (on a logarithmic scale) at various wavelengths $\lambda = 550$ nm (blue), 800 nm (black), and 1100 nm (red) for two different pulse lengths $\tau = 8$ fs (solid) and 20 fs (dashed). At very low F_0, σ is a constant dependent only on the biased DC field $F_{\rm DC}$, which is set at 0.2 V/nm (much smaller than the typical DC field used in pure field emission experiments). This explains the extremely small values of $\sigma < 10^{-13}$ nC/μm^2 at $F_0 < 0.3$ V/nm and we may consider no electron emission at all in this region for application purposes. By increasing the laser field to $F_0 > 1$ V/nm, we have electron emission in the multiphoton emission regime, which follows a scaling of $\sigma \propto F_0^{2n}$ with $n = 2$, 3, and 4 representing the number of photons required at the respective wavelengths ($\lambda = 550$, 880, and 1100 nm) to overcome the potential barrier. At these wavelengths and pulse lengths, the work function (4.5 eV) is close to a multiple of the photon energy and τ is significantly larger than the laser cycle, such that $f\tau = 2\pi c\tau/\lambda > 2.5$. Under these conditions, it is found that n is independent of the laser pulse length. For example, $n = 3$ for both $\tau = 8$ and 20 fs at the same $\lambda = 800$ nm (see black solid and black dashed lines).

On further increasing the laser field F_0 to a critical field $F_c > 5$ V/nm, the scaling of $\sigma \propto F_0^{2n}$ is no longer valid, and the emission mechanism enters the optical tunneling regime.

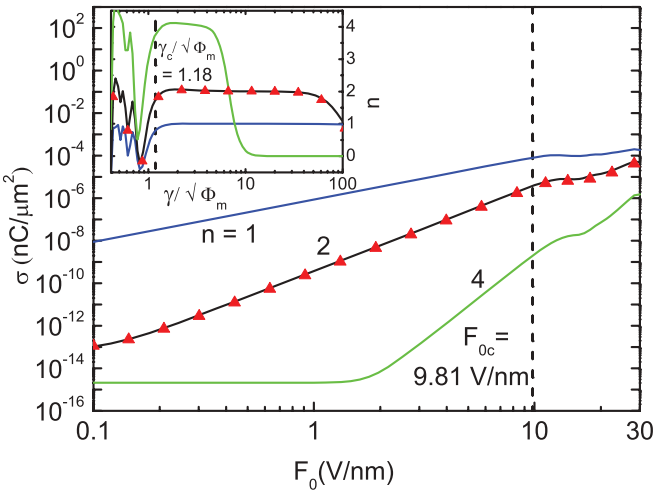

FIG. 2. (Color online) Effect of metal work function Φ_m (eV) = 2.25 (blue), 4.5 (black), and 9 (green) on the emitted charge density at $\lambda = 550$ nm. The dotted lines show the transition from multiphoton to optical tunneling regime. The inset shows the plot of n vs γ.

In order to clearly see the onset of optical tunneling from the multiphoton regime, n is plotted as a function of the Keldysh parameter given by $\gamma \approx 6356 \times \sqrt{\Phi_m}$ (eV) $\times \lambda$ (nm)$^{-1} \times F_0$ (V/nm)$^{-1}$ in the inset of Fig. 1. In this paper, the onset point is the value of γ at which n is no longer a constant and starts oscillating. It is clear that below the critical value of $\gamma_c = 2.5$ (or $F_0 > F_c$), the fitting value of n is no longer a constant, and starts to fluctuate at small $\gamma < \gamma_c$, which indicates the transition from the multiphoton regime to the optical tunneling regime.

The corresponding critical values of laser field at the transitions are $F_c = 4.90$, 6.74, and 9.81 V/nm, indicated by the vertical lines in Fig. 1. It is interesting to note, that for all four cases presented in Fig. 1, where the work function is close to a multiple of the photon energy, the transition occurs at the *same* $\gamma_c = 2.5$, independent of laser wavelength and pulse length, and only depends on the work function (see Fig. 2 below).

In Fig. 2, σ is plotted as a function of F_0 at a fixed wavelength $\lambda = 550$ nm (corresponding to a photon energy of 2.25 eV) for work functions $\Phi_m = 2.25$ eV (blue), 4.5 eV (black) and 9 eV (green). In the multiphoton regime ($F_0 < F_c$), we have multiphoton absorption with $n = 1$, 2, and 4 respectively as shown in the figure. The critical Keldysh parameter γ_c at the transition from multiphoton to optical tunneling regime is proportional to the square root of the work function, as shown in the inset which presents n as a function of $\gamma/\sqrt{\Phi_m}$. Numerically, it is found that the critical values are $\gamma_c/\sqrt{\Phi_m} = 1.18$ and $F_c = 9.81$ V/nm (see the vertical dashed lines in both the inset and main figure of Fig. 2) at $\lambda = 550$ nm. In addition, we also change the value of U_m to -9 eV (from the default -13.5 eV) for the $\Phi_m = 4.5$ eV case to check the dependence on U_m. The results (plotted with red triangles), show negligible difference compared to the default case (black solid line).

In summary, the critical Keldysh parameter at the onset of optical tunneling emission is given by a simple formula given by

$$\gamma_c = 1.18 \times \sqrt{\Phi_m \text{ (eV)}}. \quad (2)$$

Note that this formula has ignored the effects of field gradient and nonequilibrium excitation, which will be discussed in Sec. VI below. If the effect of the field gradient at different tip radii is included, it will only modify the numerical constant 1.18, as indicated by Fig. 6. The formula remains accurate for any tip with a radius r_0 larger than 80 nm. The difference is about 6 to 20% between a sharp tip (of $r_0 = 40$ to 10 nm) and a flat surface ($r_0 = \infty$, without the effect of field gradient).

IV. PULSE LENGTH DEPENDENCE OF MULTIPHOTON EMISSION

If we vary the laser wavelength λ so that the work function is *not* close to a multiple of the photon energy, our model shows that the value of n in the multiphoton regime will become sensitive to laser pulse length τ even though the number of cycles for the laser pulse remains significantly larger than 1 ($f\tau > 2.5$). Figure 3(a) shows the dependence of n on λ at $F_0 = 1$ V/nm for $\tau = 6$, 8, and 20 fs with $\Phi_m = 4.5$ eV. According to the classical photoelectric effect, the transition

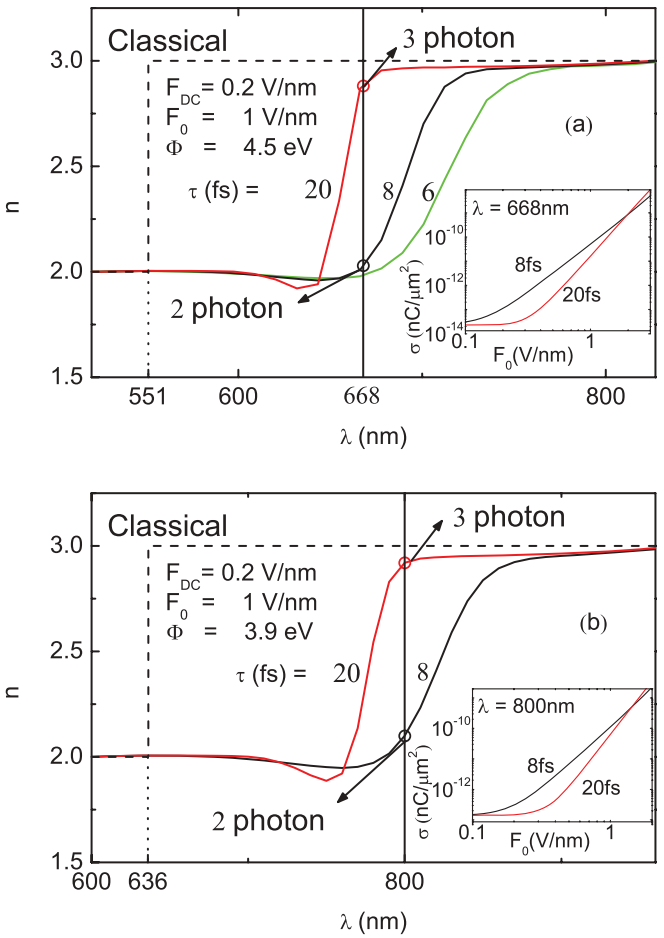

FIG. 3. (Color online) Dependence of n on laser wavelength λ at different pulse lengths τ. The vertical line shows the transition from $n = 3$ ($\tau = 20$ fs) to $n = 2$ ($\tau = 8$ fs).

from $n = 3$ to $n = 2$ for the multiphoton electron emission should occur sharply at 551 nm (dashed line). However, our model shows that a smooth transition occurs at a larger wavelength (>640 nm) with sufficient short pulse length $\tau = 6$ to 20 fs. This indicates that multiphoton electron emission can occur with fewer photon ($n = 3$ to $n = 2$) absorptions in the ultrafast time scale.

At $\lambda = 668$ nm, the photon energy is 1.86 eV, which is about 0.4 eV lower than the photon energy (2.25 eV) at 551 nm required for $n = 2$ photon absorption (according to the classical photoelectric model). In the ultrafast time scale, this deficit of 0.4 eV is supplied by the energy uncertainty principle estimated by ΔE (eV) $\approx h/\tau = 4.14/\tau$ (fs). For $\tau = 8$ fs, we have $\Delta E \approx 0.52$ eV, which is higher than 0.4 eV and thus $n = 2$ multiphoton emission is possible even at 668 nm. However for $\tau = 20$ fs, ΔE is only about 0.21 eV, which is insufficient to overcome the deficit of 0.4 eV, and thus we need $n = 3$ multiphoton absorption at 668 nm for the 20 fs case. The inset in Fig. 3(a) shows the corresponding σ ($\propto F_0^{2n}$) vs F_0 graph at 668 nm for 8 and 20 fs, which clearly shows the $n = 2$ and $n = 3$, respectively. Similarly at $\lambda = 730$ nm, the deficit is 0.55 eV which is higher than $\Delta E \approx 0.52$ eV, and thus it remains as $n = 3$ multiphoton absorption at $\lambda \geqslant 730$ nm for the 8 fs case.

To confirm this reduction from $n = 3$ to $n = 2$ by lowering the laser pulse length from 20 to 8 fs, we have purposely chosen a work function of 3.9 eV, so that the transition can occur at a wavelength of 800 nm which is common to many ultrafast laser systems. As shown in Fig. 3(b), this new work function of 3.9 eV shows a similar behavior at $\lambda = 800$ nm since the energy difference between the photon energy (1.55 eV) and photon energy required for $n = 2$ photon absorption (1.95 eV) is again 0.4 eV. Thus, we have the same reduction from $n = 3$ to $n = 2$ by lowering the laser pulse length from 20 to 8 fs, and it will be interesting to conduct an experiment to confirm this prediction. Again, the inset of Fig. 3(b) shows the σ vs F_0 graph at 800 nm for 8 and 20 fs pulses. It is important to note that this finding of anomalous multiphoton absorption is different from another experimental finding, which is due to the resonant excitation of surface plasmons at the interface between two perfect metals.[19]

V. EFFECT OF LASER PHASE AND PULSE LENGTH

In Fig. 4, we study the effects of laser phase angle $\phi = 0$ (solid lines) and $\phi = \pi$ (dashed lines) in both the multiphoton and optical tunneling regimes at $\lambda = 800$ nm for $\tau = 3$ and 8 fs. At $\tau = 8$ fs (green and blue), the number of cycles is 3 ($f\tau = 3$), and the total emitted charge density σ is independent of the phase angle in the multiphoton regime ($F < F_c = 6.74$ V/nm). On decreasing τ to 3 fs (black and red), τ becomes comparable to the laser cycle ($f\tau \approx 1$) and the emitted charge becomes phase dependent. σ for the $\phi = 0$ case (black solid line) is higher than the $\phi = \pi$ case (red dashed line), as the peak of the laser envelope coincides with a maximum of the sinusoidal term in the laser field at $\phi = 0$, for which only the region close to the middle of the laser envelope contributes to the total emitted charge density and thus σ for $\phi = 0$ is higher for 3 fs case. In the optical tunneling regime ($F > F_c = 6.74$ V/nm), σ is always phase dependent regardless of the pulse width.

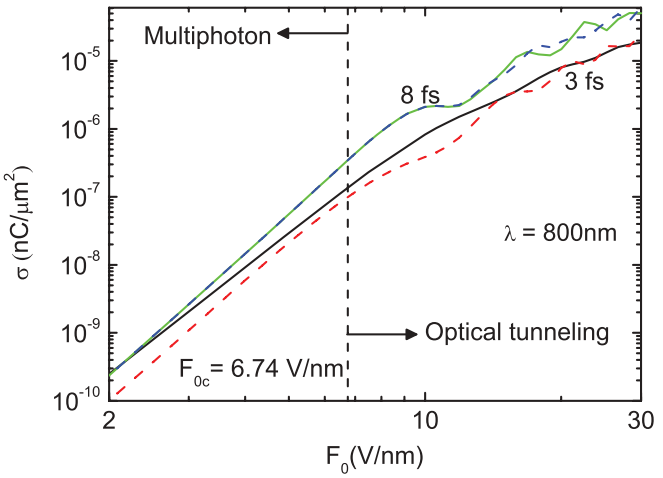

FIG. 4. (Color online) Effect of phase $\phi = 0$ (solid) and π (dashed) on the emitted charge density at $\tau = 3$ and 8 fs.

In Fig. 5(a), σ as a function of τ is plotted on a logarithmic scale in the multiphoton regime ($F_0 = 1$ V/nm) at $\lambda = 550$ nm for $\phi = 0, \pi/2$, and π. At $\tau > 4$ fs ($f\tau > 2$), we have $\sigma \propto \tau$, as the net number of incident photons is proportional to τ at fixed F_0. In this linear $\sigma \propto \tau$ regime, the time-dependent current density $J(t)$ closely follows the laser field shape as indicated in Fig. 5(b) at $\tau = 8$ and 20 fs (red and blue), and the oscillations in $J(t)$ correspond to the laser cycles. Decreasing τ to the $f\tau < 1$ region, σ will have a local minimum and then a local maximum, which are (for $\phi = 0$), respectively, around $\tau = 1.9$ fs ($f\tau \approx 1$) and $\tau = 0.3$ fs ($f\tau \approx 0.16$). In this nonlinear regime, $J(t)$ no longer follows the laser field indicated by the 1 fs case ($f\tau \approx 0.55$) in Fig. 5(b) (green).

In Fig. 5(c), we repeat the same calculations but at a different $\lambda = 668$ nm for which the work function is *not* a multiple of the photon energy. Compared to Fig. 5(a), there is an additional oscillation between $\tau = 2$ and 15 fs, and the linear $\sigma \propto \tau$ region starts later at $\tau > 15$ fs compared to $\tau > 4$ fs at 550 nm mentioned above. Thus it is expected that $J(t)$

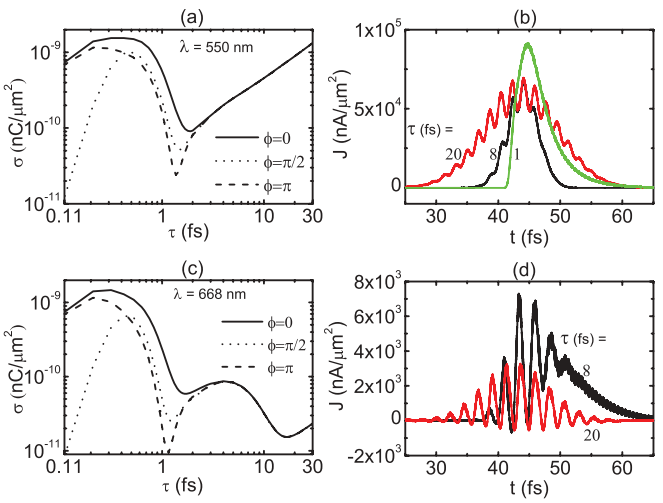

FIG. 5. (Color online) Dependence of emitted charge density σ and current density J on τ and ϕ.

closely follows the laser pulse shape for $\tau = 20$ fs (linear region) but not for $\tau = 8$ fs, which is still in the nonlinear region [see Fig. 5(d)]. This finding can also be used to explain the higher value of σ for $\tau = 8$ fs at $F_0 = 1$ V/nm as compared to $\tau = 20$ fs due to the anomalous multiphoton emission shown earlier in Fig. 3.

The effect of laser phase ϕ is very similar for both $\lambda = 550$ and 668 nm. It is clear that phase is only important when $f\tau \lesssim 1$ (i.e., τ is comparable to or smaller than the laser cycle) as in the case of $\tau < 2$ fs. The $\phi = 0$ case has the highest σ as its maximum of the laser envelope coincides with the maximum of the sinusoid in the laser field. Based on this reasoning, one would expect the $\phi = \pi$ case to have the minimum σ, which is accurate down to about $f\tau \approx 0.2$ [$\tau \approx 0.4$ fs (for 550 nm) and 0.5 fs (for 668 nm)]. At very small τ ($f\tau < 0.2$), the $\phi = \pi/2$ case has the smallest σ as the field is zero near the middle of the laser envelope and thus the field is nearly absent for extremely short pulses at this phase angle.

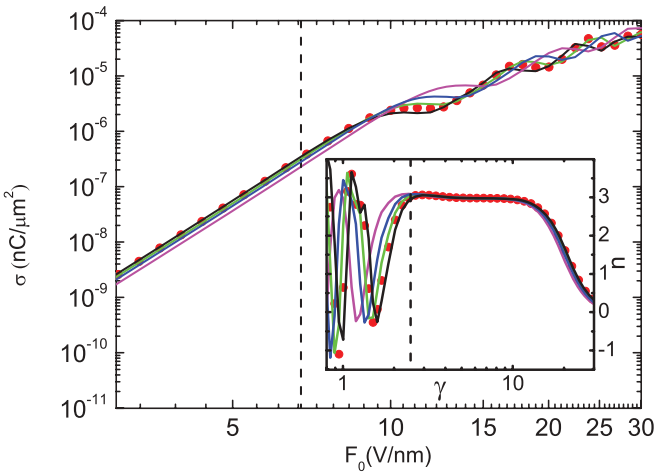

FIG. 6. (Color online) Comparison of the emission characteristics from tips with different radii of curvature.

VI. DISCUSSION

As mentioned in the introduction, there have been many interesting studies in the area of ultrafast laser-induced electron emission from a sharp tip. In this section, we will compare our work with prior works and suggest future improvements. We will start with comparing the critical Keldysh parameter (γ_c) as suggested by our formula with the corresponding reported Keldysh parameter in the transition region between the multiphoton and optical tunneling regimes from various studies. From our formula (without the effect of field gradient), the critical Keldysh parameter is $\gamma_c = 1.18 \times \Phi_m^{1/2} = 2.5$ to 2.77 for work functions of 4.5 eV (tungsten) to 5.5 eV (gold), which is inside the transition region reported by experiments,[1–4,6–8,10,11] such as strong photoemission from gold[8] ($\gamma \approx 2 < \gamma_c = 2.77$), and attosecond electron emission from tungsten[11] ($\gamma \approx 2 < \gamma_c = 2.5$) which are in the optical tunneling regime. The above-threshold photoemission from tungsten[10] ($\gamma \approx 3$ to $5 > \gamma_c = 2.5$) is in the multiphoton regime.

It is important to note that the critical Keldysh parameter reported here is at the onset of optical tunneling, which indicates the lower bound of the transition region. Thus, the value is slightly higher compared to the reported values, which are well inside in the transition region. We will use an example to illustrate the difference and also to suggest the other possible reasons for our higher critical Keldysh parameter. From Fig. 2 in a recent paper, Ref. 8, the transition from multiphoton to tunneling is smooth from 0.3 to 0.7 J, and it is hard to tell the onset position from the experimental measurement. Our prediction of $\gamma_c = 2.77$ corresponds to about 0.31 J, which is indeed at the lower bound in the transition region. Another two possible reasons that may cause the differences are the effects of field gradient[12] and nonequilibrium electron energy distribution due to laser excitation in the metal.[5]

So far in this paper, we have assumed that the electric field is spatially uniform and the effect of spatial variations in the electric field caused by field enhancement near the tip has been ignored completely. To include the effects of the field gradient near the tip, we have used the electric field profile used by Herink *et al.*:[12] $F(x) \approx F(0^+) \times [r_0/(x + r_0)]^3$ if the beam waist is large compared to the barrier width and the geometric field enhancement is significantly larger than 1, where r_0 is the radius of curvature of the tip and $F(0^+)$ is the field just outside the metal at $x \to 0^+$. These two conditions are valid in almost all experimental studies.[1–4,6–8,10–12] By integrating $F(x)$, we obtain the potential profile which is used in our time-dependent quantum model to calculate the emitted charge density σ as a function of F_0 for $r_0 = 10$ nm (magenta), $r_0 = 20$ nm (blue), $r_0 = 40$ nm (green), $r_0 = 80$ nm (red circles), and $r_0 = \infty$ (black, which is the uniform field case), as shown in Fig. 6. The inset in the figure is the corresponding n as a function of γ. Note that the selected values of $r_0 = 10$, 20, and 80 nm are based on experimental studies by Herink *et al.*,[12] Borman *et al.*[8] and Hommelhoff *et al.*[2] respectively.

At very small r_0, such as $r_0 = 10$ nm (magenta), there is a change in the curve, as the field gradient is large enough to change the emission characteristics. The actual field seen by the electron after it is emitted is smaller than F_0 and, as a result, the onset of the tunneling regime will take place at $\gamma_c \approx 2$, which is 0.5 smaller than the critical Keldysh parameter $\gamma_c \approx 2.5$ with a uniform field (black line). By increasing r_0, this effect is found to disappear very rapidly. At $r_0 = 40$ nm (green), the onset point is $\gamma_c = 2.36$, which is just 6% less than the uniform field case. At $r_0 = 80$ nm (red circle), it shows nearly no effect of the field gradient. Thus, the results of the reported figures in this paper (Figs. 1–5, 7, and 8) based on a uniform field should accurately describe tips with radius of curvature of 40 nm or greater. A detailed analysis of the effect of field gradient on emission characteristics will be the subject of future study.

In a recent paper (without field gradient) by Yalunin *et al.*[9] (see Fig. 4 in their paper), the electron emission characteristics have been calculated as a function of laser field for $\Phi_m = 5.5$ eV, $\lambda = 800$ nm, and $\tau = 30$ fs. In Fig. 7, we have repeated the same calculation based on our model and also plotted the dependence of n as a function of the Keldysh parameter in the inset of the figure. By comparing our results (blue line) and Yalunin's paper (red line), we find that both actually show that the onset of the optical tunneling regime is around $\gamma_c = 1.18 \times \Phi_m^{1/2} \approx 2.77$. Because the image charge

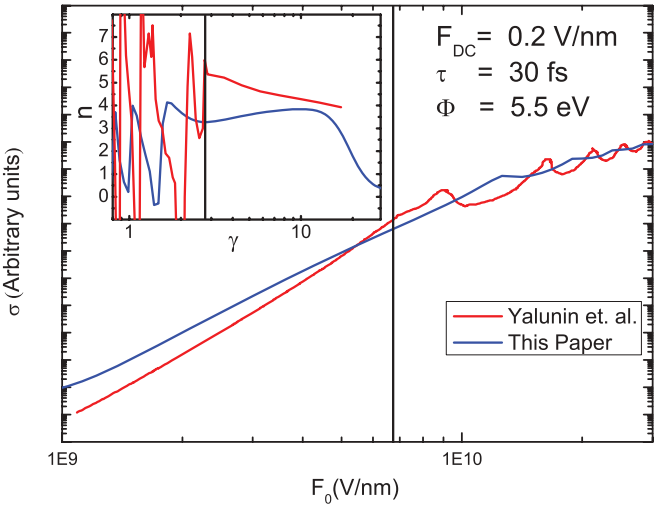

FIG. 7. (Color online) Comparison of the model from this paper with the model of Yalunin *et al*. (Ref. 9). The difference between the two models arises because of the lack of image charge in Ref. 9.

has not been taken into account in Yalunin's model,[9] there is a difference between the two results, and the n from Yalunin's model is not perfectly constant even in the multiphoton regime. However, it can be seen that the start of the fluctuations for both curves in the inset is consistent with $\gamma_c = 1.18 \times \Phi_m^{1/2} \approx 2.77$. Since the paper by Yalunin *et al*.[9] claims to agree well with experimental results,[8] we are confident that our prediction of $\gamma_c = 2.5$ to 2.77 at the onset of optical tunneling is within the range of experimental results due to reasonable agreement between the two models as shown in Fig. 7.

One limitation of our model is that the nonequilibrium electron energy distribution caused by ultrafast laser excitation has not been taken into account, for which the effective work function for electrons to tunnel through may be reduced due to higher electron energy. At much lower laser field <1 V/nm, this mechanism has been studied in our prior paper[5] and it is also confirmed by recent experiments.[6,7]

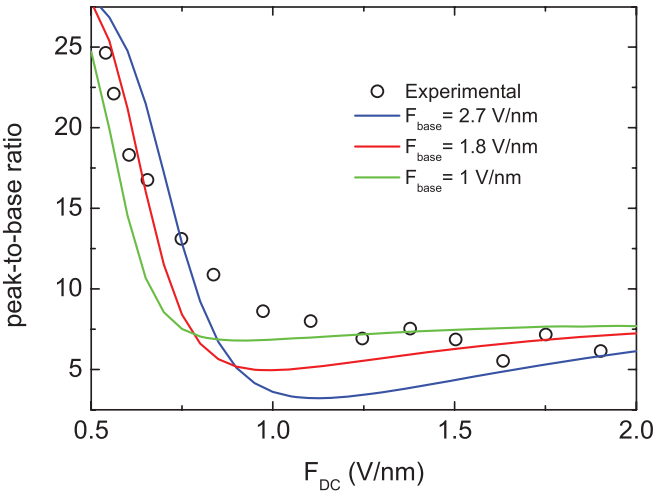

FIG. 8. (Color online) Comparison of the peak-to-base ratio from the model with experimental results from Ref. 2.

The future inclusion of the nonequilibrium electron excitation process with the time-dependent tunneling model reported here would provide a more accurate description of the transition region between the multiphoton and tunneling regimes. While it is beyond the scope of this paper, we will make a simple argument on the reduction of $\gamma_c = 2.5$ towards $\gamma_c = 2$ if the excitation process is considered. If we assume an average of one photon absorbed per electron during the excitation process, the emission energy is increased by one photon, and the effective work function will be decreased by one photon energy, which is about 2.95 eV. Interestingly, with a revised $\Phi_m = 2.95$ eV, our formula gives $\gamma_c = 1.18 \times \Phi_m^{1/2} \approx 2$, which is now inside the smooth transition regime shown in Fig. 2 reported by the recent study.[8] Thus we speculate that the formula proposed here [Eq. (2)] may remain valid to account for the effect of laser excitation on metal if an effective work function value is used for Φ_m.

Finally, we would like to compare our calculated results with an earlier experiment measuring the peak-to-base ratio of electron emission.[2] The comparison is shown in Fig. 8 for different laser fields of 1 to 2.7 V/nm with experimental measurements (open circles). The best fit is obtained with a base laser field of 1.8 V/nm if optical tunneling is the only process. Note that good agreement can also be explained by using the nonequilibrium excitation model at a much lower laser field =0.3 V/nm as shown in Fig. 5 in our prior paper.[5] Thus it is clear that, to have a detailed understanding of ultrafast laser induced electron emission from a *sharp* tip near the transition region between the multiphoton and optical tunneling regimes, it is important to include the above three effects (time-dependent tunneling, nonequilibrium excitation, and field gradient) into a consistent model, which will be studied in the near future.

VII. SUMMARY

We have obtained a critical Keldysh parameter $\gamma_c = 1.18\sqrt{\Phi_m}$ (eV) at the onset of optical tunneling, which depends only on the work function Φ_m, and is also valid for a tip with a radius of 40 nm or larger. For smaller tip radius (down to 10 nm), there will be a deviation of up to 20% compared to calculations including the effect of field gradient near to the tip. It is also speculated that the formula will remain valid to account for the effect of laser excitation on metal if an effective work function value is used for Φ_m. When the work function is *not* a multiple of photon energy, the number of photons required for multiphoton emission depends on the laser pulse length τ due to the energy uncertainty principle. The findings reported here also suggest that measuring the dependence of emitted charge on laser phase will be able to distinguish the emission mechanism. Comparisons with prior calculated and experimental results are presented and discussed.

ACKNOWLEDGMENTS

This work was supported by Singapore MOE Grant No. 2008-T2-01-033, USA ONRG Grant No. N62909-10-1-7135, and AFOSR AOARD Grant No. 11-4069.

*ricky_ang@sutd.edu.sg

[1]P. Hommelhoff, Y. Sortais, A. Aghajani-Talesh, and M. A. Kasevich, Phys. Rev. Lett. **96**, 077401 (2006).
[2]P. Hommelhoff, C. Kealhofer, and M. A. Kasevich, Phys. Rev. Lett. **97**, 247402 (2006).
[3]C. Ropers, D. R. Solli, C. P. Schulz, C. Lienau, and T. Elsaesser, Phys. Rev. Lett. **98**, 043907 (2007).
[4]B. Barwick, C. Corder, J. Strohaber, N. Chandler-Smith, C. Uiterwaal, and H. Batelaan, New J. Phys. **9**, 142 (2007).
[5]L. Wu and L. K. Ang, Phys. Rev. B **78**, 224112 (2008).
[6]H. Yanagisawa, C. Hafner, P. Dona, M. Klockner, D. Leuenberger, T. Greber, M. Hengsberger, and J. Osterwalder, Phys. Rev. Lett. **103**, 257603 (2009).
[7]H. Yanagisawa, M. Hengsberger, D. Leuenberger, M. Klockner, C. Hafner, T. Greber, and J. Osterwalder, Phys. Rev. Lett. **107**, 087601 (2011).
[8]R. Borman, M. Gulde, A. Weismann, S. V. Yalunin, and C. Ropers, Phys. Rev. Lett. **105**, 147601 (2010).
[9]S. V. Yalunin, M. Gulde, and C. Ropers, Phys. Rev. B **84**, 195426 (2011).
[10]M. Schenk, M. Kruger, and P. Hommelhoff, Phys. Rev. Lett. **105**, 257601 (2010).
[11]M. Kruger, M. Schenk, and P. Hommelhoff, Nature (London) **475**, 78 (2011).
[12]G. Herink, D. R. Solli, M. Gulde, and C. Ropers, Nature (London) **483**, 190 (2012).
[13]A. H. Zewail, Annu. Rev. Phys. Chem. **57**, 65 (2006).
[14]K. L. Jensen, J. Appl. Phys. **102**, 024911 (2007).
[15]J. P. Girardeau-Montaut, C. Girardeau-Montaut, S. D. Moustaizis, C. Fotakis, Appl. Phys. Lett. **64**, 3664 (1994).
[16]J. P. Girardeau-Montaut, C. Girardeau-Montaut, Phys. Rev. B **51**, 13560 (1995).
[17]Y. S. Tergiman, K. Warda, C. Girardeau-Montaut, J. P. Girardeau-Montaut, Opt. Commun. **142**, 126 (1997).
[18]C. Tomas, E. Vinet, J. P. Girardeau-Montaut, Appl. Phys. A **68**, 315 (1999).
[19]J. Kupersztych and M. Raynaud, Phys. Rev. Lett. **95**, 147401 (2005).